Electronic Supplementary Material (ESI) for Materials Horizons.
This journal is © The Royal Society of Chemistry 2019

Supporting Information

A cephalopod-inspired self-healable mechanoluminescence material with skin-like self-healing and sensing properties

*Quanquan Guo†, Bingxue Huang†, Canhui Lu, Tao Zhou, Gehong Su, Liyang Jia, Xinxing Zhang**

State Key Laboratory of Polymer Materials Engineering, Polymer Research Institute of Sichuan University, Chengdu 610065, China.

E-mail: xxzwwh@scu.edu.cn, canhuilu@scu.edu.cn

Table of contents

Experimental Section

Materials. Epoxidized natural rubber (ENR) latex with an epoxidation degree of 50% (solid content: 28.91 wt%) was provided by the Agricultural Products Processing Research Institute, Chinese Academy of Tropical Agricultural Science, Zhanjiang, P.R. China. Water-soluble organic fluorescent agents with different fluorescence under ultraviolet light were obtained from Shenzhen Tounaozhifu Technology Co., Ltd (China). Multiwall carbon nanotubes (CNTs) were purchased from Chengdu Organic Chemicals Co., Ltd, Chinese Academy of Sciences. Medical purified cotton was supplied by Xuzhou Health Factory Co., Ltd (China). 3-aminophenylboronic acid (APB) and 3-carboxylphenyl boronic acid (CPB) were purchased from Aladdin Regent Co., Ltd (Shanghai, China). PDMS (Sylgard 184) was obtained from Dow Corning, Inc. (USA). Sulfuric acid and other chemical reagents were all purchased from Chengdu Kelong Chemical Reagent Company (China). All reagents and ingredients were used without further purification.

Preparation of self-healable fluorescent elastomers. First of all, 10.38 g ENR latex (containing 3 g ENR) was mixed with 5 wt% APB and stirred at room temperature to dissolve modifiers. After reacting at 100 ^{o}C for 3 h, a S-ENR latex was obtained via the ring-opening reaction between epoxy groups in ENR chains and amino groups in APB molecules. For further characterization, S-ENR elastomers were obtained after removing excess water of S-ENR latex in electric oven. Then, the water-soluble fluorescent agent was blended with the functional ENR latex (mass ratio = 1:100) and intensively stirred at room temperature to prepare fluorescent S-ENR (FS-ENR) latex. After dried in electronic oven, FS-ENR elastomers with distributed fluorescence networks could be obtained. For comparation, CPB-crosslinked ENR with single dynamic crosslinking network were obtained with same procedures.

Preparation of CNC@CNTs nanohybrids. Cellulose nanocrystal (CNC) was prepared by hydrolyzing cotton with sulfuric acid according to our previous studies.[1] Briefly, medical purified cotton (20 g) was mixed with sulfuric acid solution (64 wt%, 400 mL) and heated at 45 ^{o}C for 45 min. Then, in order to avoid further hydrolysis, the reaction was immediately quenched by the dilution with deionized water.

The obtained reaction product was washed twice with deionized water by centrifugation at 5000 rpm for 5 min and then dialysis operation was applied to remove residual acid until the dialysate appeared neutral. Next, 0.10 g of CNTs was mixed with a well-dispersed aqueous suspension of CNC (containing 0.20 g of CNC) and diluted to form a 200 mL dispersion. After sonicated for 30 min at room temperature, a uniform aqueous CNC@CNTs nanohybrid suspensions was obtained.

Fabrication of cephalopod skin-like multifunctional flexible device. The cephalopod skin-like multi-functional flexible device was prepared via transfer process, as illustrated in Figure S8a. Initially, a thin UV-shielding film (5 μm) consisting of CNC@CNTs nanohybrids was prepared by drop-coating or spray-coating CNC@CNTs suspension on a pre-cleaned glass foundation. A liquid FS-ENR latex was then cast atop the thin film and then dried to form a thick self-healable fluorescent layer (50 μm). Next, a layer of S-ENR (500 μm) was added to package the fluorescent layer and increase tensile resilience via drop-coating process. The material was then carefully peeled away from the glass foundation along one direction. After carefully peeling away from the glass foundation, the morphology of the UV-shielding layer exhibited many microcracks perpendicular to the peeling direction. Finally, after encapsulated by the PDMS matrix, a multifunctional flexible device can be obtained. Moreover, the mechanoluminescence materials can be further applied in encryption field. An optional fluorescent pattern can be sandwiched between UV-blocking and S-ENR layer (Figure S8b). The hidden information can be reversible concealed upon stretching and releasing the encrypted device (Figure S8c). For preparing strain and humidity sensor, the sensing materials were coated with conductive silver paste at two ends to eliminate the contact resistance. Then, the silver pastes were connected with copper wires. Finally, PDMS was used to package the as-prepared sensor.

Characterization and analysis. FTIR spectroscopy was recorded from 4000 to 700 cm^{-1} on a Nicolet 6700 spectrophotometer (USA) at room temperature. XPS was collected on a XSAM 800 spectrometer (KRATOS, U.K.). DSC of all supramolecular elastomer was characterized using Q2000 modulated differential scanning calorimeter. (TA Instruments, USA). The morphology of the CNC@CNTs nanohybrids was studied by a Dimension 3000 AFM microscope (Digital Instruments). Zeta potentials

and particle size distributions of CNC@CNTs nanohybrids with different mass ratios were measured using a Zetasizer nano-ZS apparatus (Malvern, U.K.). Water contact angles of CNC@CNTs nanohybrids were measured at room temperature using a Drop-shape Analyzer DSA25 (KRUSS, Germany). Scanning electron microscopy (SEM) was carried out on a microscope (JEOL JSM-5900LV, Japan). LSCM (LSM700 Carl Zeiss, Germany) was carried out to detect the structural evolution of the microcrack-structured conductive shielding layer and the variation of fluorescence intensity during stretching. All of the mechanoluminescence properties experiments were performed in an ultraviolet viewing system with an ultraviolet light source of 365 nm for photographing and videotaping.

Temperature-dependent FTIR spectroscopy. Supramolecular molecular with 5 wt% APB was chosen for temperature-dependent FTIR tests. A Nicolet iS50 Fourier transform spectrometer (U.S.A.) equipped with a deuterated triglycine sulfate (DTGS) detector was used for the temperature-dependent FTIR experiments from 25 to 220 ^{o}C with a heating rate of 3^{o}C/min. All 89 FTIR spectra were collected from 4000-400 cm^{-3} and used for further analysis.

Mechanical property tests. Mechanical properties measurement was performed on a universal tensile testing machine (Instron-5560, USA) with an extension rate of 100 mm min^{-1} at room temperature. For self-healing mechanical property test, the samples were cut into a totally separated pieces by a razor blade and then put together to fully healing at room conditions.

Fluorescent property tests. The 1D fluorescence spectra of the as-prepared fluorescent materials were recorded on a FluoroMax 4 spectrofluorometer (Horiba Jobin Yvon, France) with an excited light source of 365 nm. 3D fluorescence spectra were collected from 400 to 800 nm under continuous excited wavelength ranging from 300 to 400 nm.

Sensing property tests. The sensing performance of multifunctional device was recorded in real-time by a two-point measurement with a Keithley 2601B source meter (USA) under a constant voltage of 6 volts. For human motion detection, the conductive samples were mounted on the throat and face of a volunteer to monitoring the subtle muscle motions. Then the current signal variations were recorded by the source meter.

Experiments involving human subjects. All the sensing experiments in Figure 5 were performed in compliance with the relevant laws and the approval of the Scientific Committee of Polymer Research Institute of Sichuan University. The consent of all participants involved in the sensor experiments has been obtained.

Supporting Tables

Table S1. Dissipated energy of neat ENR and S-ENR with different APB mass ratio during the load-unload cycle.

Samples	ENR	1%	3%	5%
Dissipated energy (KJ/m^3)	10.79±0.31	9.55±0.06	10.18±0.07	13.10±0.13

The energy dissipation during the load-unload cycles was measured on the universal tensile testing machine and summarized in Table S1. Both pure ENR and S-ENR samples display hysteresis and permanent residual strain behaviors. The energy dissipation during the load-unload cycles can be attributed to the dynamic covalent and hydrogen bonds fracture. As shown in the Table S1, the energy dissipation of S-ENR samples increases with increasing the APB contents, due to the higher supramolecular crosslinks constructed by the synergistic boroxines and hydrogen bonds.

Table S2. The mechanical properties of S-ENR after self-healing.

	Tensile strength (MPa)	Elongation at break (%)	Toughness (MJ/m^3)	Self-healing efficiency (%)
Original S-ENR	1.86±0.15	413.61±22.78	3.80±0.44	-
1st healed S-ENR	1.84±0.13	395.28±12.51	3.44±0.23	91
2nd healed S-ENR	1.58±0.07	402.22±20.23	3.20±0.38	84
3rd healed S-ENR	1.61±0.09	426.67±11.10	3.10±0.16	82
5th healed S-ENR	1.55±0.14	408.61±17.16	2.98±0.21	78
10th healed S-ENR	1.27±0.16	391.39±13.56	2.82±0.32	74

Supporting Figures

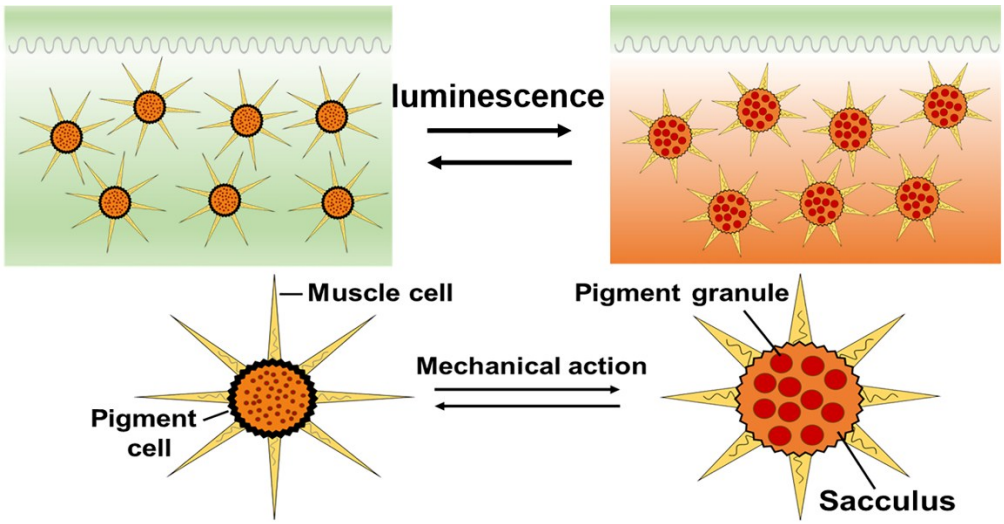

Figure S1. The responsive luminescence and coloration mechanism of cephalopod skins.

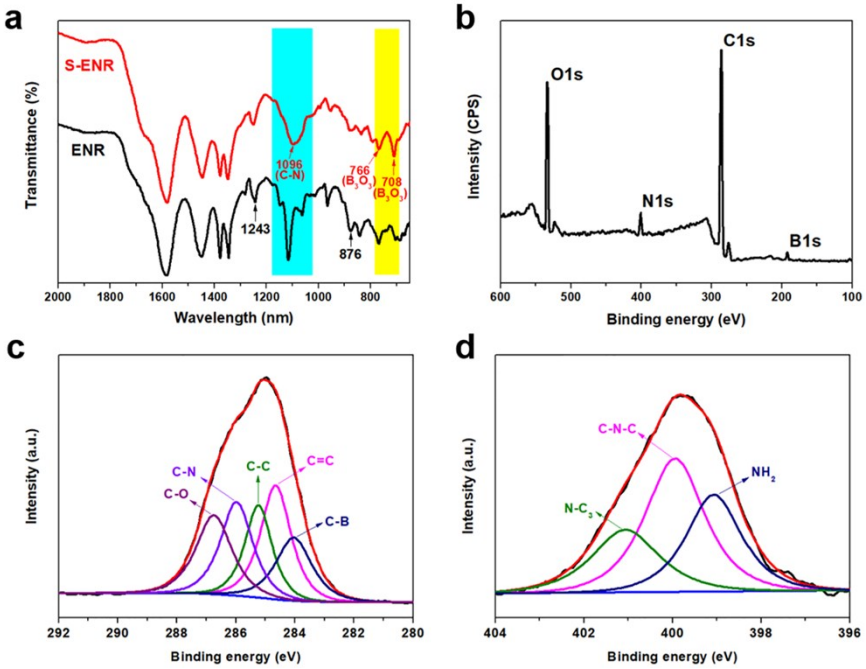

Figure S2. a) FTIR spectra of ENR and boroxines-crosslinking ENR elastomer. b) XPS survey spectra of S-ENR. c, d) The high-resolution C1s and N1s XPS spectra of S-ENR, respectively.

The grafting reactions between APB and ENR and the formation of dynamic-covalent boroxine bonds are explicitly confirmed by FTIR and XPS measurements. In the pristine ENR, the characteristic absorption peaks at approximately 1243 and 876 cm^{-1} belong to epoxy groups.[2, 3] After reacting with APB, the absorption intensities of epoxy groups decrease and the characteristic aliphatic amine absorption peak at 1096 cm^{-1} appears, indicating the consuming of epoxy groups and the successful reaction between APB and ENR (Figure 5a).[4, 5] Moreover, the XPS spectrum of S-ENR shows the peaks of B 1s and N 1s, ascribed to the B and N elements presenting in S-ENR (Figure 5b). The chemical structure variation was revealed by the different chemical states of C and N. The C 1s core-level spectrum could be curve-fitted with five peak components, including 286.6 (C-O), 285.9 (C-N), 285.2 (C-C), 284.6 (C=C) and 284.0 (C-B) eV, respectively.[6, 7] The appearance of C-N and C-B bonding indicates the inclusion of APB molecules in ENR chains. In addition, the N 1s core-lever spectrum can be divided to three main peaks at 401.1, 400.0 and 399.1 eV, which are assigning to the $N-C_3$, C-N-C and $-NH_2$, respectively.[8] These results demonstrate the successful ring-opening reaction between epoxy groups in ENR and amino groups in APB molecules.

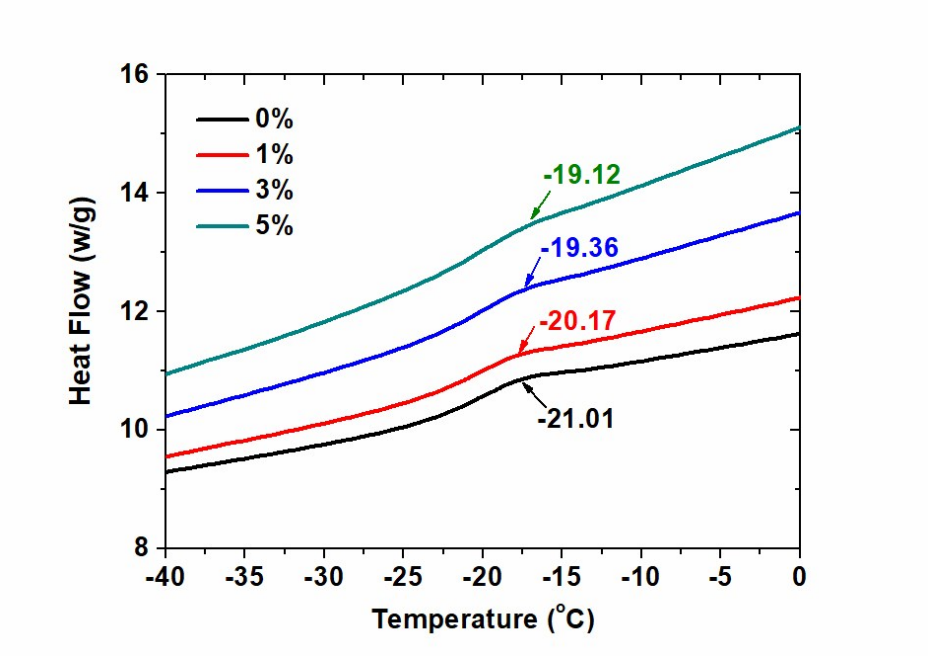

Figure S3. Differential scanning calorimetric study of synergistic dynamic crosslinked ENR with different 3-aminophenylboronic acid content. As shown in the Figure S3, the glass temperature (*Tg*) of neat ENR in DSC is measured to be -21.01 °C. After introducing 1 wt% APB, the Tg is shifted to -20.17 °C. And the *Tg* of supramolecular elastomer increases with the increasing of APS content, indicating the presence of dynamic interactions among ENR chains.

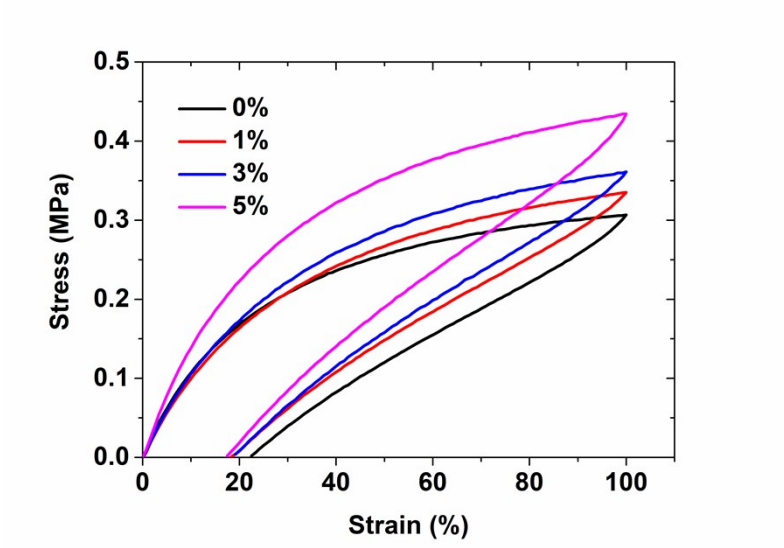

Figure S4. The hysteresis loops of neat ENR and S-ENR with different APB content. Both pure ENR and S-ENR samples exhibit evident hysteresis owing to the presence of the synergistic boroxines and hydrogen bonds.

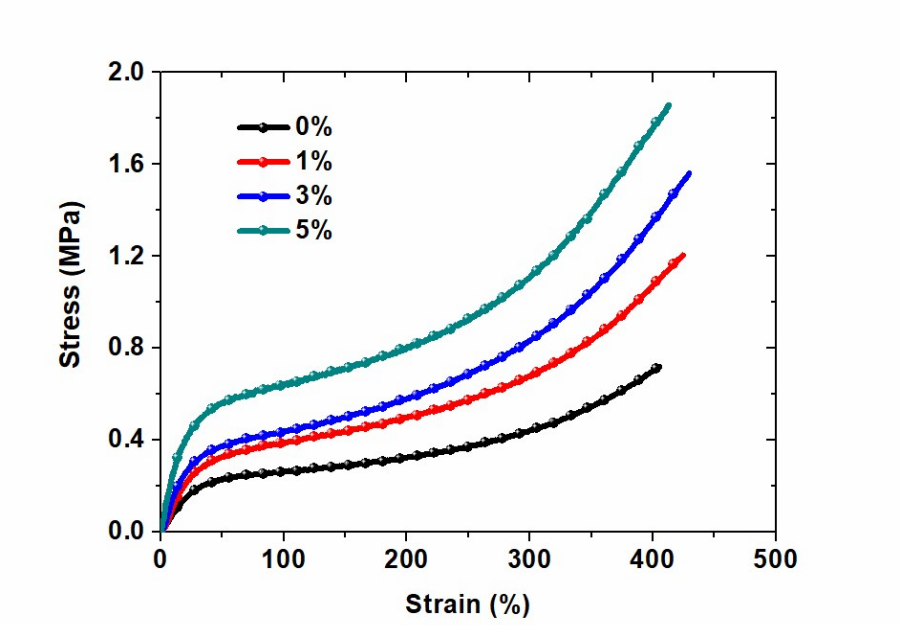

Figure S5. Stress-strain curves of S-ENR samples with different APB mass ratios. The tensile strength of S-ENR elastomers increases monotonously with increasing ABA content owing to the presence of dynamic crosslinking network can effectively dissipate energy. Notably, the tensile strength and modulus of S-ENR elastomers are significantly improved without sacrificing the extensibility. It can be ascribed to the dynamic and reversible nature of dynamic-covalent boroxine and hydrogen bonds, which render the unfolding and sliding of the polymer chains during stretching and thereby improve stretchability of the elastomer.

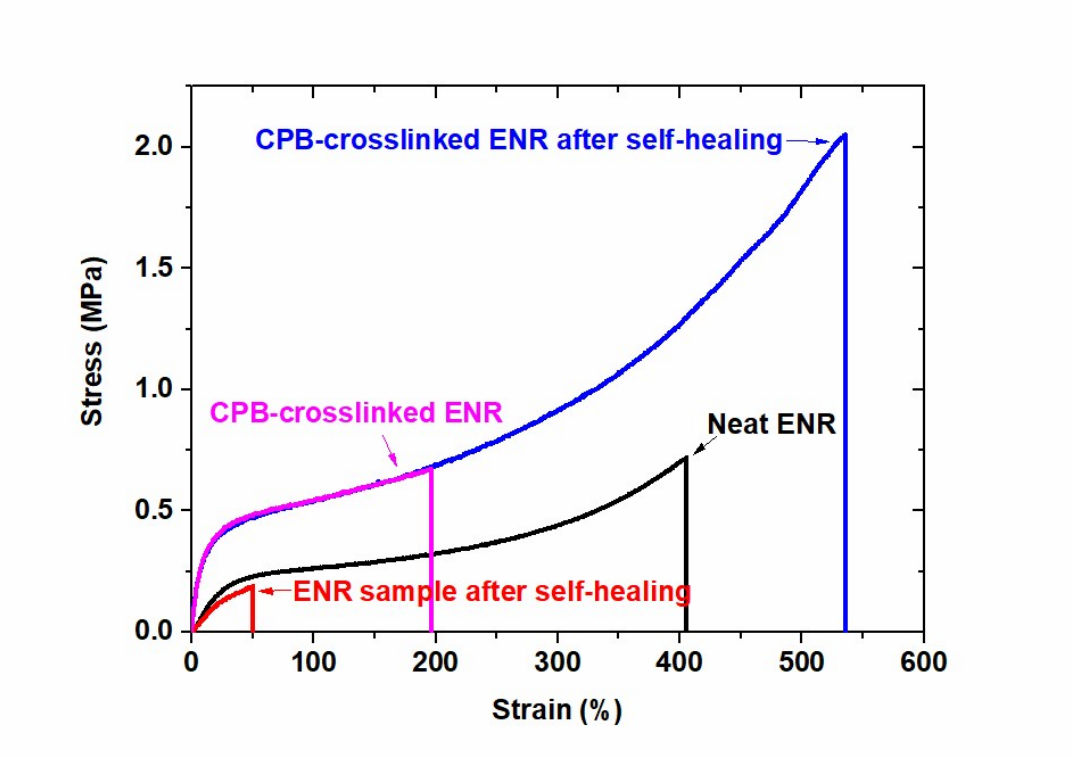

Figure S6. Stress-strain curves of neat ENR and 3-carboxylphenyl boronic acid-crosslinked ENR samples after self-healing. Neat ENR can only heal about 25% of its original mechanical strength (0.19 MPa) owing to the entanglement of rubber chains. The single dynamic covalent-crosslinked ENR exhibit a poor healed mechanical strength of 0.67 MPa after healing at room temperature.

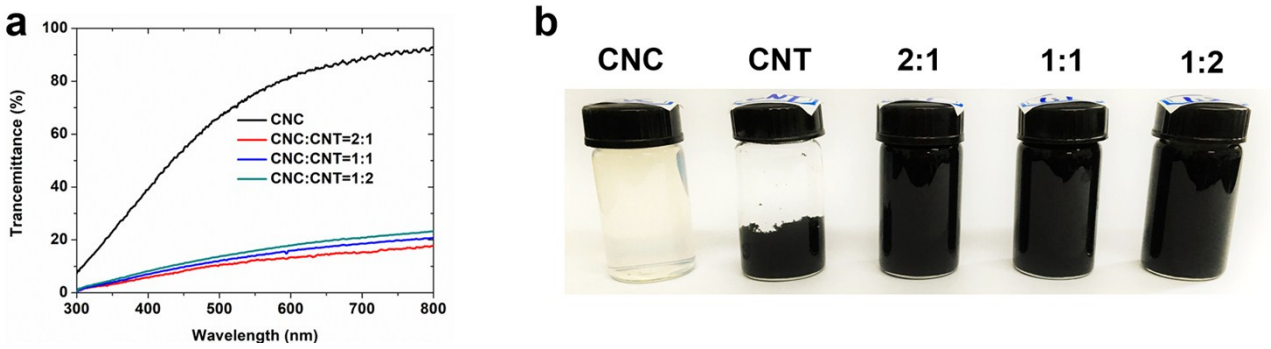

Figure S7. (a) The ultraviolet absorption spectra of CNC@CNTs nanohybrids with different mass ratio. The presence of CNTs can effectively block UV-light via absorption (b) Digital pictures of CNC@CNTs nanohybrids after placing one month. No evident aggregation phenomena of CNC@CNTs nanohybrids can be observed, while pure CNTs have been totally sedimented, indicating excellent water dispersion and stability of our prepared nanohybrids.

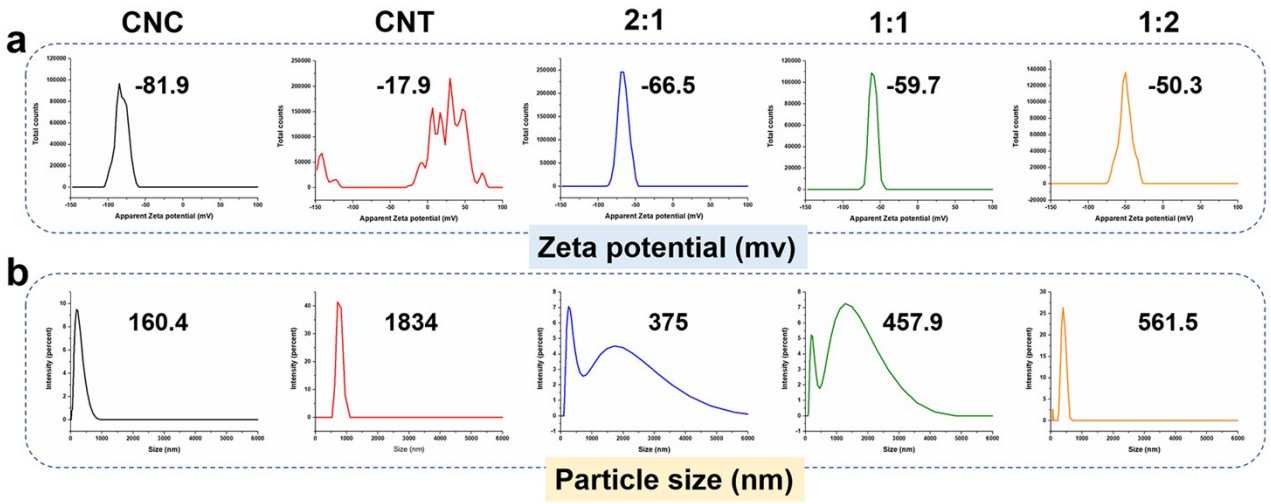

Figure S8. a) Zeta potential and b) particle size distribution of CNC, CNT, CNC@CNTs nanohybrids with a mass ratio of 2:1, 1:1, 1:2.

Zeta potential and particle size analysis were carried out to investigate the physical properties of CNC@CNTs nanohybrids. As shown in Fig S, the neat CNTs dispersion with a Zeta potential of -17.9 mV shows poor suspension stability, which are liable to form precipitate in aqueous solution. With the inclusion of CNC, the nanohybrid exhibits good suspension stability, as confirmed by the Z-potential of different CNC@CNTs nanohybrids which are below -30 mV.[9] In addition, the particle size of aggregated CNTs (average size of 1834 nm) sharply decreases after forming CNC@CNTs nanohybrids, indicating that CNC can effectively disperse CNTs in aqueous solution and thereby greatly improve the water-suspension of CNTs.

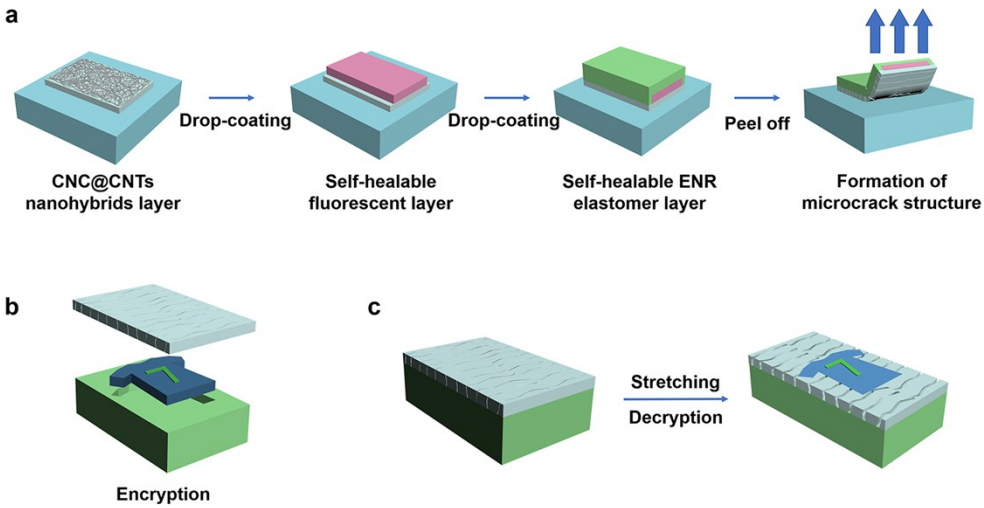

Figure S9. a) Preparation scheme of versatile cephalopod skin-like material and b, c) its encryption application.

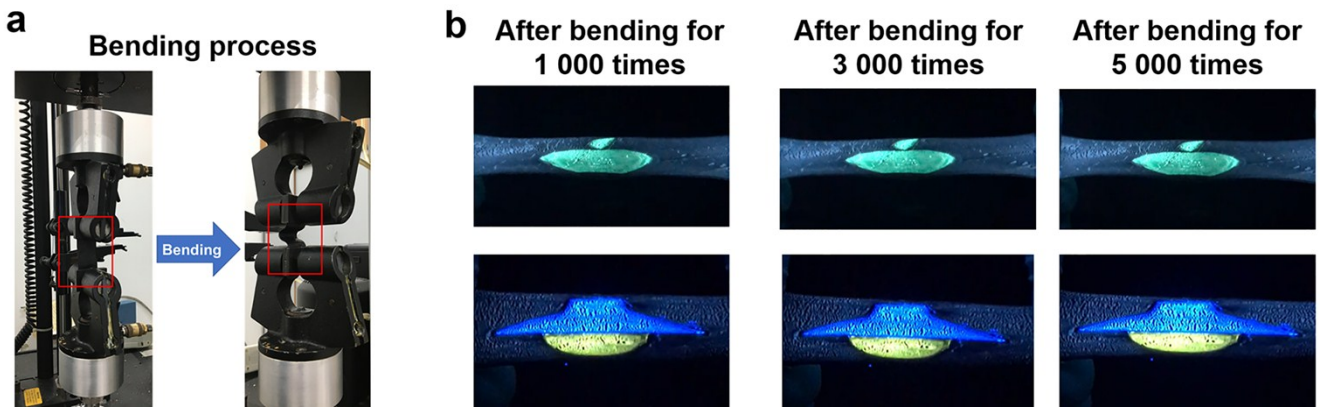

Figure S10. a) The digital pictures of mechanoluminescence samples during bending process on a universal tensile testing machine. b) The healed encrypted patterns concealed at stretching state after bending for 1 000, 3 000, 5 000 times.

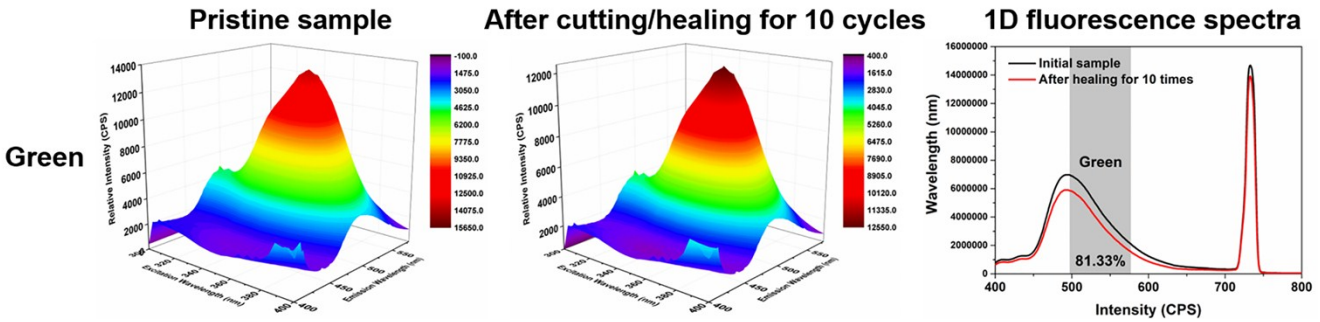

Figure S11. The 3D and 1D fluorescence spectra of green-fluorescence sample after healing for 10 times.

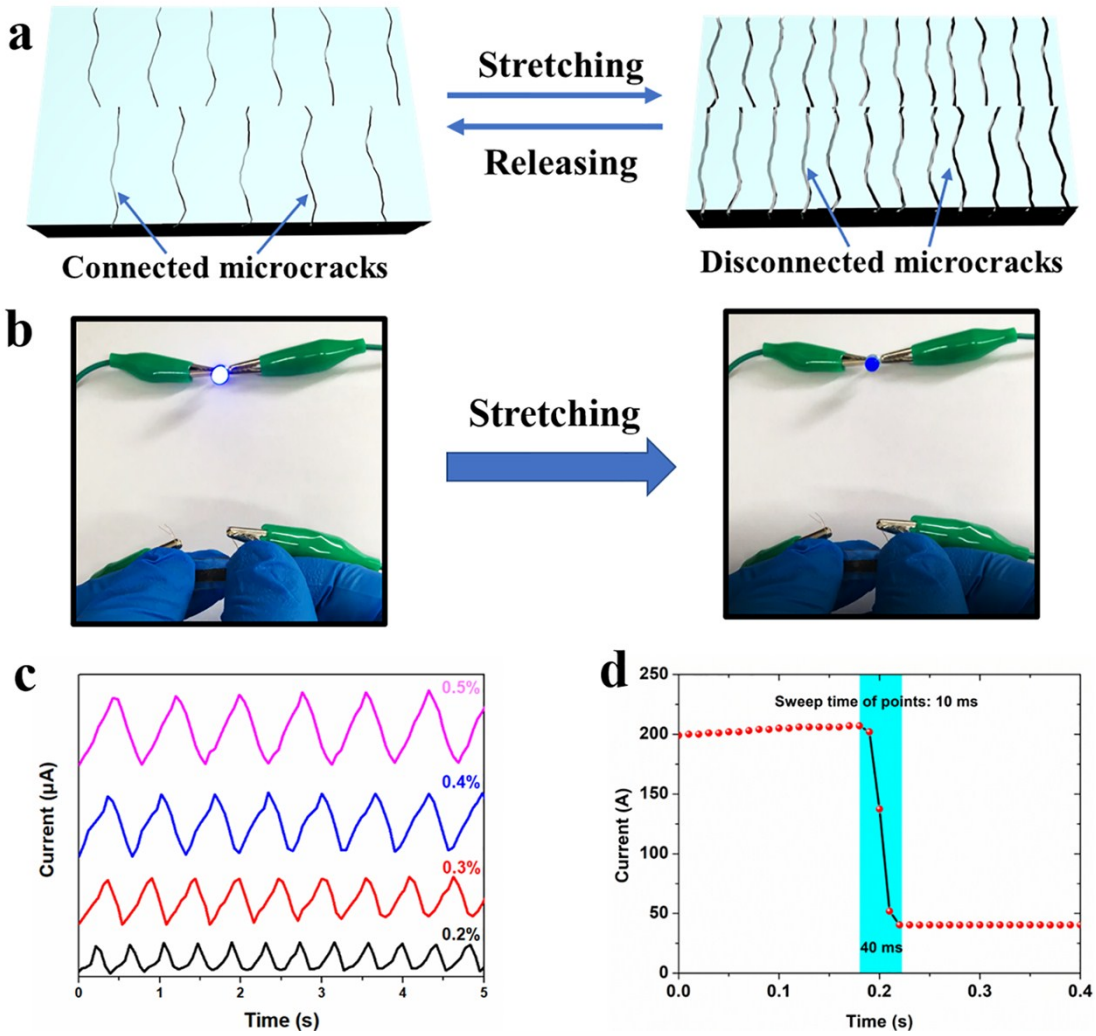

Figure S12. a) Schematic variations of microcracks under deformation in conductive UV-shielding layer. b) Demonstration of strain-responsive conductive ability of the versatile device when connected into a circuit with an LED light. c) The responsive current changes under different tensile strains at cyclic tests. d) Instant response of our versatile device under a sweep time of 10 ms, which shows a response time of 40 ms.

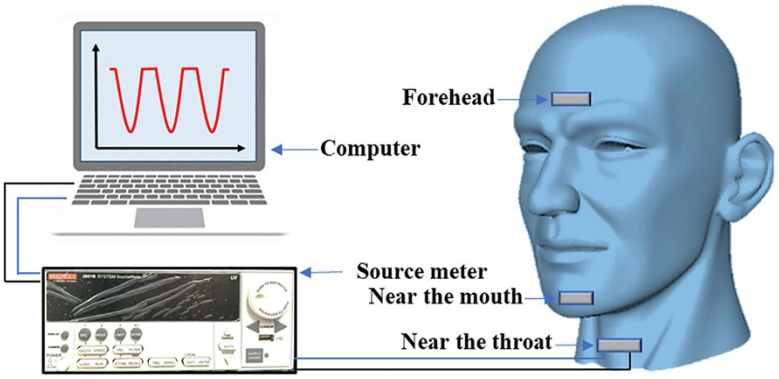

Figure S13. Schematic illustration of the speech and expression recognition based on our versatile device.

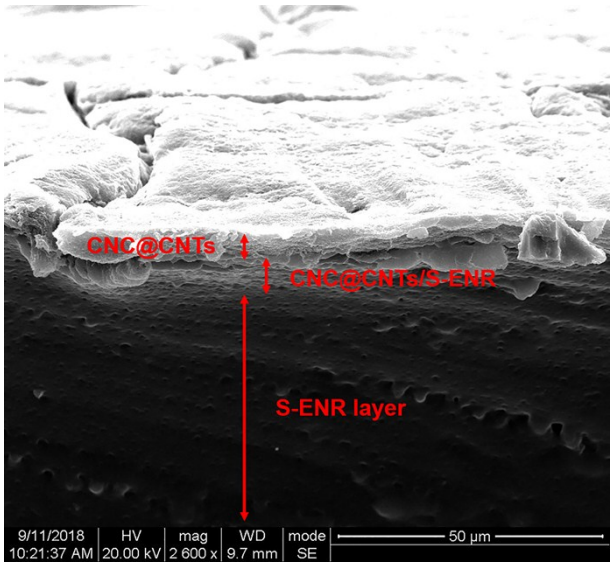

Figure S14. SEM image of the fracture surface of as-prepared electronic sensor.

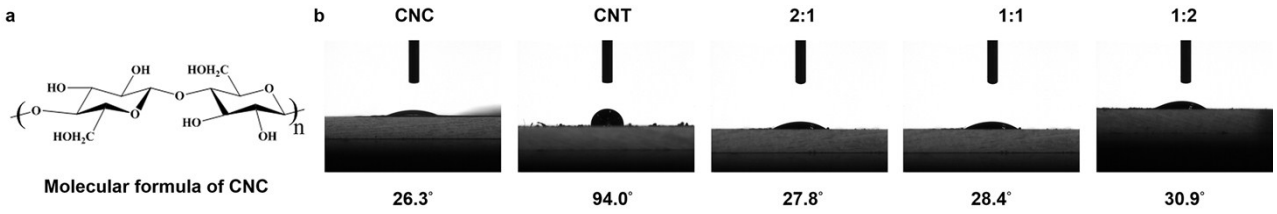

Figure S15. a) Molecular formula of CNC. b) Water contact angle variation of CNC@CNTs films with different mass ratios. After introducing of CNC, the water contact angle of CNTs changed from 94.0° to 27.8°, illustrating the hydrophilic properties of CNTs are greatly improved.

Reference

1. S. Wang, X. Zhang, X. Wu and C. Lu, *Soft mater*, 2016, **12**, 845.

2. A. J Van Zyl, S. M. Graef, R. D. Sanderson, B. Klumperman and H. Pasch, *J. Appl. Polym. Sci.*, 2003, **88**, 2539.

3. C. T. Ratnam, M. Nasir, A. Baharin and K. Zaman, *Polym. Int.*, 2000, **49**, 1693.

4. P. A. Angeli Mary and S. Dhanuskodi, *Cryst. Res. Technol.*, 2001, **36**, 1231.

5. J. E. Stewart, *J. Chem. Phys.*, 1959, **30**, 1259.

6. Y. Jiang, M. Wei, J. Feng, Y. Ma and S. Xiong, *Energy Environ. Sci.*, 2016, **9**, 1430.

7. G. Chen, J. Qiu, J. Xu, X. Fang, Y. Liu, S. Liu, S. Wei, R. Jiang, T. Luan, F. Zeng, F. Zhu and G. Ouyang, *Chem. Sci.*, 2016, **7**, 1487.

8. F. Arcudi, L. Đorđević and M. Prato, *Angew. Chem. Int. Edit.*, 2016, **55**, 21.

9. J. D. Clogston and A. K. Patri, *Characterization of nanoparticles intended for drug delivery*, Humana Press, 2011, **697**, 63.